ROYAL SOCIETY OPEN SCIENCE

royalsocietypublishing.org/journal/rsos

cc BY

Research

Cite this article: Kumar N, Jensen HJ, Viegas E. 2026 Tracing inequitable emissions in global trade using a networks approach. *R. Soc. Open Sci.* **13**: 251246.
https://doi.org/10.1098/rsos.251246

Received: 5 July 2025
Accepted: 28 October 2025

Subject Category:
Science, society and policy

Subject Areas:
complexity, mathematical modelling, graph theory

Keywords:
network science, international trade networks, emissions, inequity, directed networks

Author for correspondence:
Nishanth Kumar
e-mails: nishanthk050@gmail.com; nk821@ic.ac.uk

Tracing inequitable emissions in global trade using a networks approach

Nishanth Kumar[1], Henrik Jeldtoft Jensen[1,2] and Eduardo Viegas[1,2]

[1]Centre for Complexity Science and Department of Mathematics, Imperial College London - South Kensington Campus, London, UK
[2]School of Computing, Institute of Science Tokyo, Yokohama 226-8503, Japan

NK, 0000-0001-6889-7844; HJJ, 0000-0002-5398-3288

Do patterns of international trade align with the distribution of emissions embodied in trade? In this paper, we use methods from network science to present a descriptive analysis of the alignment between bilateral international trade and the emissions embodied in the trade flows across countries and sectors between 1995 and 2020. By constructing and comparing weighted trade and emissions networks over this period, we quantify the dissimilarities between economic value and environmental cost. We provide insights into how this dissimilarity varies across key economic sectors and over time. Beyond documenting this imbalance, we explore the structural properties of the trade and emissions networks, revealing contrasting patterns of assortativity and 'rich-club' formation. Specifically, we find that trade flows exhibit a persistent concentration among developed nations. This is notably absent in emissions, where environmental burdens are more diffused across countries. We introduce a simple measure of 'inequity' both at the local and global level, based on the disproportionate emissions intensity of trade flows. Our findings show that these inequities are not randomly distributed but are strongly patterned by income: lower-income countries are consistently found to be emission-intensive exporters to wealthier economies. This partition, persistent across time and sectors, highlights a fundamental asymmetry in the environmental costs of global trade.

1. Introduction

The advent of globalization has dramatically increased the interdependence in production and economic activity across the world, reshaping how countries, firms and individuals engage in economic exchanges. Production processes became fragmented and modularized to capitalize on lower labour costs and resource

THE ROYAL SOCIETY PUBLISHING

© 2026 The Authors. Published by the Royal Society under the terms of the Creative Commons Attribution License http://creativecommons.org/licenses/by/4.0/, which permits unrestricted use, provided the original author and source are credited.

Downloaded from http://royalsocietypublishing.org/rsos/article-pdf/doi/10.1098/rsos.251246/5646930/rsos.251246.pdf
by guest
on 27 June 2026

availability. The expanding network of production and supply means that a single product may be designed in one country, manufactured in another with components sourced from multiple locations and then sold globally.

Consequently, economic activities in one part of the world can have far-reaching effects, influencing job markets, wages and economic growth in distant countries [1]. Disproportionate gains for rich countries from activities that have led to global warming have been evidenced. At the same time, poorer economies have suffered disproportionately from the effects of global warming [2,3].

A recent paper [4] argues that poor countries have been made poorer (in relative terms) by the energy consumption of wealthy countries. The cited research estimates that the top 10% of the richest population contributes to nearly half of the total emissions, while the bottom 50% contribute to about 12%. This is not as stark a picture as that of wealth inequalities where the top 10% of the richest population own more than 75% of the wealth [5]. Empirical analyses for the period between 1961 and 2010 showed that countries contributing the least to emissions suffered the most negative economic effects, and the countries who contributed the most to emissions all had a median economic growth of more than 10% [2]. The most recent figures from the global carbon budget estimate that emissions in 2023 have decreased by 7.4% in the European Union and by 3.0% in the United States, but have increased by 4.0% in China and 8.2% in India [6]. There is an argument that the wealthiest and most developed countries gained more by industrialization and have since begun to decouple their emissions from growth.

International trade has been well studied using networks to infer the structural patterns, hierarchy and the interdependencies in global trade. Several studies [7–11] have revealed that these networks exhibit scale-free and small-world characteristics, with strong disassortativity in their binary or unweighted form. When extending this to weighted networks, the dissortative tendencies are weakened [12], which indicates that high-volume trade tends to occur between similarly large economies. In [11], the authors show that although a 'rich-club' structure, where strong nodes interact more intensively with each other, has been present but is weakening over time. This trend reflects the growing integration of developing countries into global trade networks and the diminishing dominance of traditional economic powers in controlling trade exclusively among themselves.

More recently, with access to detailed data on emissions embodied in trade—defined as the emissions generated during the production of goods and services that are subsequently traded—we are able to extend these models to study environmental externalities alongside economic flows. It is important to note that in such networks, emissions do not literally 'flow' between countries; rather, the networks trace the movement of goods whose production caused emissions in the exporting country. Emissions embodied in trade are a notional construct, linking environmental effects to international bilateral trade. Building on this conceptual foundation, several recent studies have applied network approaches to emissions data to reveal how trade redistributes environmental burdens globally. For instance [13], used multi-regional input-output analysis to show that high-income countries tend to outsource significant portions of their carbon footprints to emerging economies through imports. In [14], this idea was extended to methane emissions, finding that over a quarter of global anthropogenic methane emissions are trade-related, with China, the USA and Russia acting as central nodes in a core-periphery structured methane flow network. Similarly, Guidi *et al*. [15] demonstrated a persistent global flux of CO_2 emissions from net exporters of emissions (often less 'carbon-efficient' economies) to net importers of emissions (typically wealthier, more efficient countries), despite improvements in individual countries' carbon intensities.

In this article, we present a descriptive, comparative analysis using methods in complexity and network science that quantifies and tracks the dissimilarity between international trade and the emissions embodied in those flows across countries and sectors. The core aim is to highlight the emerging patterns of inequitable trade among countries emerging in the context of trade and embodied emissions.

We use only the patterns of bilateral trade and their intensities (both capital and emissions) to measure dissimilarity. To do this, we normalize trade and emissions data and build two undirected weighted networks: the weighted trade network (WTN) and the weighted emissions embodied in trade network (WEETN). We compare these networks using correlation and mutual information measures. We also disaggregate the data into three economic sectors and compare how dissimilarities vary across sectors and over time (1995–2020). These findings are presented in §2.1. Second, in §2.2, we explore how node strengths and link weights scale in the WTN and WEETN. We focus on how trade and emissions flows differ by sector and analyse patterns of assortativity and scaling between node-level and edge-level quantities. Third, in §2.3, we introduce a null model that generates synthetic networks with similar statistical properties. By comparing the real network to this benchmark, we identify structural features—such as

Downloaded from http://royalsocietypublishing.org/rsos/article-pdf/doi/10.1098/rsos.251246/5646930/rsos.251246.pdf
by guest
on 27 June 2026

rich-club dynamics—that go beyond random expectations. Finally, in §2.4, we turn to the directed versions of the WTN and WEETN, which capture the direction of trade flows. We construct a new network, G^{EI}, based on emissions intensity (i.e. emissions per unit trade). Using this, we assess inequity both locally (at the node and edge levels) and globally (using trophic structure). We quantify the directionality of inequitable flows and their alignment with income levels.

Here, we note that inequity specifically refers to the disproportionalities in flows of trade and corresponding emissions embodied in trade. We include a more general discussion on inequity and how results validate a deeper study of mechanisms leading to inequitable norms of this type in §4. It is important to note that in this article, the terms misalignment and dissimilarities refer to statistical divergences, computed through correlation coefficients and mutual information.

2. Results

In the following sections, we refer to undirected versions of the WTN and WEETN by $\tilde{G}^T$ and $\tilde{G}^C$, respectively. We refer to the directed versions by G^T and G^C. We refer to the directed network of emission intensity by G^{EI}.

2.1. The weighted trade network and the weighted emissions embodied in trade network

Using the OECD's Inter-Country Input–Output (ICIO) tables [16,17] and the OECD's TECO2 database [18,19], we construct two weighted networks: (i) WTN (G^T), where each node represents a country and each edge captures the total value of goods and services exchanged (in USD) and (ii) WEETN (G^C), where edges represent the total greenhouse gas (GHG) emissions embodied in trade (in tonnes of CO_2-equivalent).[1] The flows of emissions embodied in bilateral trade are measured in tonnes of CO_2 equivalent (tCO2e) which expresses the quantity of GHGs released in terms of carbon dioxide (CO_2) [19]. To simplify the analysis, we look at the networks aggregated, with the undirected trade volume as the edge weight. For a meaningful comparison, we normalize the edge weights by the total trade volume in the network, resulting in the edge weights being a share of the total trade volume. See §3.1 for more on the construction of the networks.

The two networks are similar by nature of their construction. The links in the WEETN represent the emissions embodied in bilateral trade, which means that if there is a link between two nodes i and j in the WTN, then there will also be a link between i and j in the WEETN. Given the normalization of the edge weights in $\tilde{G}^T$ and $\tilde{G}^C$ to represent the share of global trade volume and share of emissions embodied in global trade, respectively, the networks are similar. Note that $\tilde{G}^X$ refers to the symmetric, undirected network representing trade volumes, where as G^X represents the directed network.

In figure 1a, we visualize the WTN for the year 2019 after applying a connectivity-preserving threshold: all edges with weights below a threshold value w_0^T are removed, where w_0^T is the largest value that retains a connected network. For 2019, this results in $w_0^T = 0.0001$, yielding a sparser network that preserves global connectivity while retaining approximately only the top 25% of the original links.

The WTN reveals a well-connected core of countries through which the largest trade volumes flow. Figure 1a provides a snapshot of this structure in 2019. Since the corresponding emissions network (WEETN) exhibits a similar topology, owing to the nature of emissions being embedded in traded goods, we highlight in figure 1b the deviations between the two. Here, each edge reflects the difference in normalized weights between trade value and embodied emissions. This highlights asymmetries: whether a trade involves a disproportionately high monetary value relative to its emissions footprint, or vice versa. In simple terms, the edges on the network in figure 1b highlight the misalignment in the financial and environmental costs of the transaction. We observe red edges connecting the USA with countries such as China, India and Vietnam, indicating trade relationships where the emissions embodied in trade exceed the monetary value. Conversely, blue edges appear between the USA, Japan and several major European countries, suggesting trade links where monetary value dominates relative to the emissions exchanged.

To explore this dissimilarity in more detail, we compare the bilateral weights of the WTN and the WEETN by estimating the correlation coefficients. We compute the Pearson correlation coefficient (r) and the Spearman rank correlation coefficient (ρ) for the year 2019. We find that $r = 0.94$ and $\rho = 0.97$ both indicate a strong positive relationship between trade and emissions flows. This suggests that, overall, countries that trade more also tend to be associated with higher emissions in trade. We know that

[1]These emissions account for the entire lifecycle of traded goods, including production, transportation and delivery.

Downloaded from http://royalsocietypublishing.org/rsos/article-pdf/doi/10.1098/rsos.251246/5646930/rsos.251246.pdf
by guest
on 27 June 2026

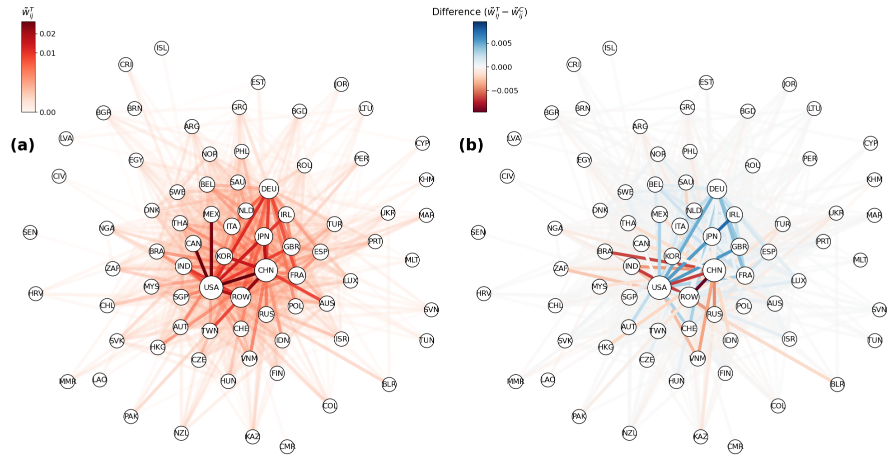

Figure 1. The WTN and its difference with the WEETN in 2019: (a) The normalized WTN, where the thickness and opacity of each edge reflect the bilateral trade volume as a share of global trade. Node sizes are proportional to the total trade strength of each country. (b) The difference network showing the disparity between trade and emissions embodied in trade (WEETN), with edge colours representing the signed difference $\tilde{w}^T ij - \tilde{w}^C ij$. Red edges indicate that the emissions embodied in trade exceed the corresponding trade volume for that link, while blue edges indicate the opposite. Colour intensity and opacity scale with the magnitude of this difference. Both plots show approximately 25% of the edges where $w^T_{ij} > 0.0001$ which is chosen, is the maximum threshold value such that we have a connected network.

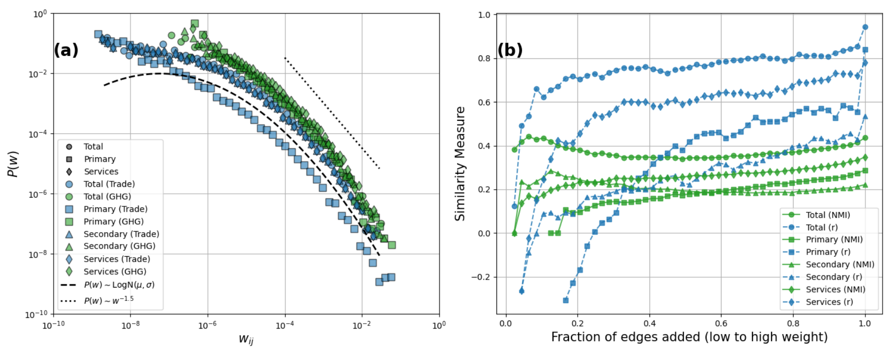

Figure 2. Link weight distribution and similarity measures for WTN and WEETN across sectoral classifications in 2019: (a) Empirical distributions of edge weights for the trade and GHG networks across economic sectors (Total, Primary, Secondary, Services) in 2019. Distributions are shown on a log-log scale. A log-normal fit is overlaid for the Total Trade sector, along with a power-law tail with exponent −1.5 (b) Cumulative similarity between trade and GHG networks as a function of the fraction of edges (ordered by average weight). Both Pearson correlation and NMI are computed incrementally, highlighting how similarity evolves as increasingly stronger links are included. Markers and colours distinguish sectors and network types

the distribution of edge weights is heavy-tailed and follows broadly a log-normal distribution, as seen in figure 2a. The high correlation values could be biased by the larger edge weights. If the two networks both assign higher weights to the same country pairs but differ significantly in how weight is distributed among medium or low-weight edges, the correlations would still be high and unable to capture deviations across the entire distribution. To complement these, we compute the normalized mutual information (NMI), which compares the informational similarity between the distributions of weights. Given two discrete random variables X and Y (in our case, the binned logarithmic weights of WTN and WEETN). High correlation implies similar global patterns; high NMI would imply deeper structural similarity, whereas low NMI indicates potential mismatches in how trade and emissions are distributed, even if globally they look similar.

There is dissimilarity between WTN and WEETN. While both r and ρ indicate strong linear and rank-based correlations, respectively, the NMI reveals a more nuanced picture. In particular, the correlation survival function shows that the strength of correlation between the two networks declines sharply after removing the top k% of edges, suggesting that the apparent similarity is dominated by a small subset of high-weight links. The NMI highlights these subtler mismatches in edge weights and remains around 0.42 in 2019, despite increasing over time.

Downloaded from http://royalsocietypublishing.org/rsos/article-pdf/doi/10.1098/rsos.251246/5646930/rsos.251246.pdf
by guest
on 27 June 2026

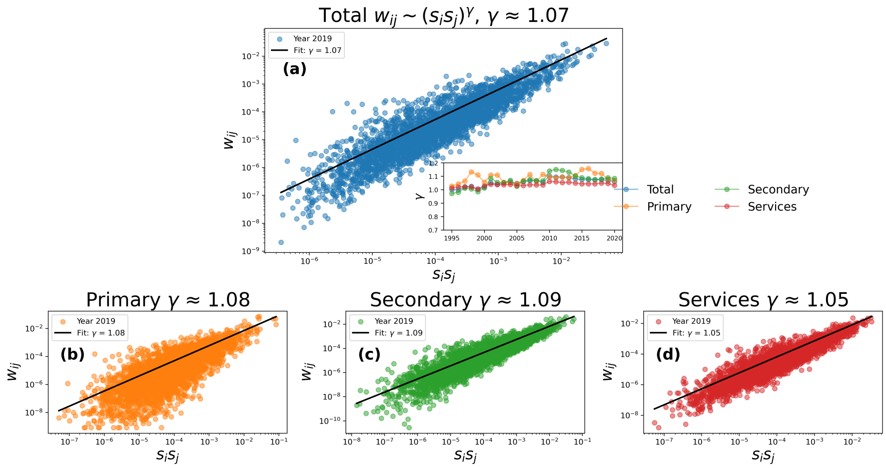

Figure 3. Relationship between node strength and edge weights in the WTN in 2019: (a) For each network, the link weight w_{ij} is plotted against the product of node strengths $s_i s_j$, showing a positive correlation indicative of assortative mixing. A power-law fit $w_{ij} \sim s_i s_j$ is applied, with the exponent γ indicating the scaling behaviour. The inset shows the evolution of γ over time for each sectoral classification. (b–d) Comparison across sectors: primary, secondary and services.

This persistent asymmetry implies that, even though the overall topology and strongest trade relations are similar, the distributions of monetary trade values and embodied emissions differ significantly—indicating that trade flows in dollars and in emissions do not align uniformly across the network.

We decompose the total bilateral trade among the countries into three broad sectoral classifications: Primary, Secondary and Services. The primary sector includes activities such as agriculture, fishing and extraction of natural resources (such as mining and quarrying). The secondary sector includes activities that are related to manufacturing, such as chemicals, metals, machinery, food processing and energy production. Finally, the services sector or the tertiary sector includes a wide range of activities such as construction, trade, transport, communication, finance, public administration, education, health care, etc. The full classification can be found in appendix A.

The NMI is consistently higher for the networks constructed using the total trade volume than for any of the individual sectors. This suggests that while individual sectors may exhibit greater variation between trade and emissions flows, the aggregate network smooths out these discrepancies. Dissimilarities present in one sector may be offset or diluted by patterns in others, leading to a higher similarity score when all sectors are considered together.

2.2. Assortativity in the weighted trade network and the weighted emissions embodied in trade network

We proceed to examine the relationships between node strengths and link weights to understand the assortativity in the WTN and WEETN. Given that the networks have a link density of approximately 1, we look to the strengths of nodes $s_i = \sum_j w_{ij}$, which is the total trade the country is involved in. We consider the relationship between node strengths and link weights by fitting the relationship $w_{ij} \sim (s_i s_j)^{\gamma}$, where s_i and s_j are the strengths (i.e. total weighted degree) of the nodes and w_{ij} is the weight of the link connecting them. The exponent γ captures how pairwise node strength relates to the magnitude of their interaction. We fit γ for the WTN and WEETN for the year 2019 in figures 3 and 4, respectively.

The exponent γ tells us how strongly connected nodes relate to one another. A higher γ means strong nodes tend to connect more intensely. In the total, secondary and services sectors, γ values are similar between the trade and emissions networks. This suggests that emissions follow trade patterns closely in these sectors. However, in the primary sector, γ is much higher for trade (1.08) than for emissions (0.82). This means that strong trade connections do not correspond to equally strong emissions links. Emissions are more unevenly spread in the primary sector, showing a mismatch between trade volume and environmental effect. The inset in figure 4a shows that these relationships are quite stable over time and that this mismatch in the primary sector has persisted throughout the period of our analysis from 1995 to 2019. If γ is significantly lower in the WEETN than in the WTN, it suggests that while strong economies trade heavily with each other (high γ in WTN), the flow of emissions is more diffused than the flow of

Downloaded from http://royalsocietypublishing.org/rsos/article-pdf/doi/10.1098/rsos.251246/5646930/rsos.251246.pdf
by guest
on 27 June 2026

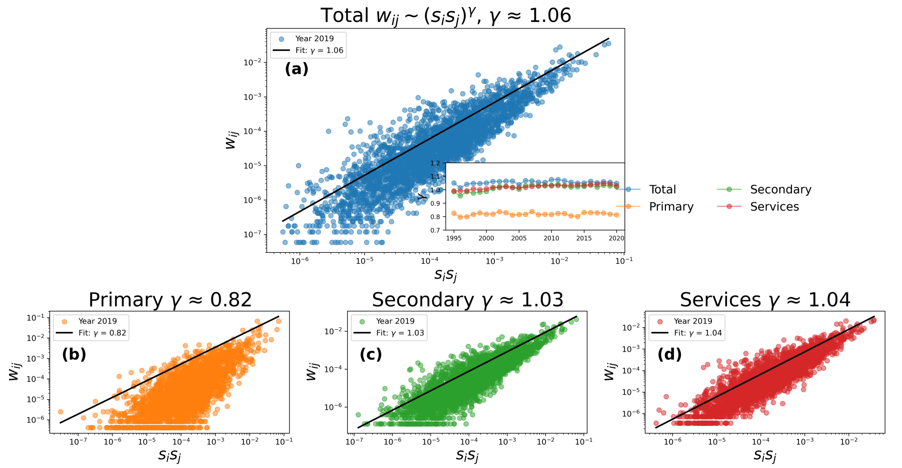

Figure 4. Relationship between node strength and edge weights in the WEETN in 2019: (a) For each network, the link weight w_{ij} is plotted against the product of node strengths $s_i s_j$, showing a positive correlation indicative of assortative mixing. A power-law fit $w_{ij} \sim s_i s_j$ is applied, with the exponent γ indicating the scaling behaviour. The inset shows the evolution of γ over time for each sectoral classification. (b–d) Comparison across sectors: primary, secondary and services.

trade in monetary terms. This divergence is a potential signal of asymmetry—where emissions-intensive production is relocated to less economically dominant countries. In simple terms, this divergence suggests a pattern where countries with high trade volumes tend to trade more among themselves, while emissions associated with that trade are disproportionately directed toward countries with lower overall trade activity.

2.3. Weighted rich-club coefficient of weighted trade network and the weighted emissions embodied in trade network

The value of γ tells us that the link weights scale with the strength of the nodes, giving us an average global correlation between these quantities and also a measure of assortivity in these networks. In many real-world cases, we have seen the existence of a rich-club within the network. The rich-club effect refers to the tendency of nodes with high strength—that is, countries with large total trade volumes—to form a densely interconnected core. In the context of global trade networks, this reflects whether the most economically active countries tend to trade intensively among themselves. By measuring the rich-club coefficient, given in equation (3.3), we can better understand the concentration of trade among the nodes. This has been done for trade networks previously under different conditions [11]. In the context of our analysis, a comparison of this effect between the WTN and WEETN could offer insight into the concentration of the two networks and their sectoral counterparts and reveal structural differences.

The common choice for a null model would be a maximally random network, which preserves the degree or strength sequence (i.e. marginals) while randomizing the rest of the links. However, in the context of trade networks, this assumption may be overly simplistic. Empirical evidence from our analysis—particularly the scaling relationship between link weights and node strengths captured by the exponent γ—suggests the presence of preferential attachment, where nodes with high strength are more likely to form strong connections. This observation is consistent with findings in the literature and reflects an underlying tendency for dominant trading countries to attract a disproportionate share of global trade. Therefore, rather than comparing the observed network against an uninformed random baseline, we adopt a more realistic null model that incorporates principles of preferential attachment. By using a null model that already includes the effect of strength (through preferential attachment), we can control for that basic tendency. Then, if we still observe a rich-club effect beyond what the model predicts, it suggests there is something more going on—like a deliberate or emergent pattern where central countries form tightly knit, exclusive groups. This would reflect deeper organization in the network, not just the outcome of random connections weighted by strength.

There are several well-studied null models for international trade networks [20,21]. We use the model detailed in [22] as a null model. This is a stochastic generative model of the WTN, referred to as *SynthTrade*, which is based on a preferential attachment mechanism on the selection of both the importer

Downloaded from http://royalsocietypublishing.org/rsos/article-pdf/doi/10.1098/rsos.251246/5646930/rsos.251246.pdf
by guest
on 27 June 2026

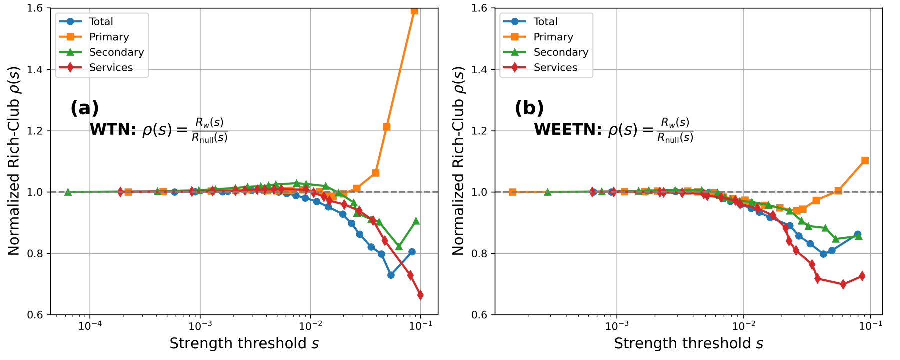

Figure 5. Normalized rich-club coefficient for WTN and WEETN in 2019: (a) The left-hand panel shows the $\rho(s)$ for the WTN in 2019, indicating how pronounced the rich-club effect is compared to the null model that already employs a strength-based preferential attachment mechanism described in section (d). Different colours and markers highlight different sectoral classifications. (b) The right-hand panel shows the same for the WEETN for 2019, offering a comparison of $\rho(s)$ for the two networks.

and exporter. The model produces weighted and directed networks based on a stochastic process that iteratively places tokens (representing units of trade or emissions) from exporter countries to importer countries based on probabilities of exporters and importers being chosen independently. A detailed summary of the model can be found in §3.4. We also offer a small modification of the model by introducing gravity-like exponents to the probabilities of choosing importers and exporters. We show that the null model provides a good fit of the marginal distributions (node strengths) and link weight distribution of the data in appendix D, which makes it a good null model to test against when studying structural features like the rich-club coefficient.

The values of $\rho(s)$ in figure 5a,b for the WTN and WEETN, respectively, reveal some differences in the interactions and the organization of high-strength nodes in the WTN and WEETN. In both networks, we see that $\rho(s) \approx 1$ for lower strength thresholds (up to $s \approx 10^{-2}$), indicating no significant deviation from the null model. However, beyond this point, we begin to see some divergence from the null model. In the WTN, we see that there is a decline in $\rho(s)$, suggesting that countries with high trade volume are weakly interconnected when compared to the null model. The effect is most pronounced in the total network, followed by services and then secondary. The WTN for the primary sector shows a sharp increase with $\rho(s) > 1$ for large s. This indicates that high-strength countries in the primary WTN are more strongly interconnected than expected under a preferential attachment-based null model.

The WEETN also shows similar behaviour of divergence at higher strength thresholds (s) where $\rho(s) < 1$ indicating high-strength nodes are weakly interconnected. Among them, the services sector shows the sharpest decline, suggesting a notably dispersed pattern of emissions flows at the top end of the network. The secondary sector follows similar trajectories, with less pronounced but still clear suppression of rich-club organization. Interestingly, the primary sector behaves differently from the WTN counterpart. It oscillates closer to 1, with negative for values $s > 10^{-2}$ before going above 1 for the largest strength threshold.

The substantially higher ($\rho(s)$) values for the primary sector in the WTN compared to the WEETN suggest a structural asymmetry between trade and emissions networks. In the WTN, strong nodes within the primary sector are tightly interconnected, forming a rich club that facilitates intensive exchange of primary goods. However, this cohesion is not mirrored in the emissions network, where these same nodes do not exhibit similarly dense emissions flows. This divergence implies that while high-strength countries engage heavily in primary sector trade with one another, the associated emissions may be externalized or distributed, potentially reflecting practices such as outsourcing or offshoring.

2.4. Measuring inequity in weighted trade network and the weighted emissions embodied in trade network

For the directed case of the WTN and WEETN, noted by G^T and G^C, the measures of similarity in table 1 are consistently lower than the undirected, symmetric networks. The lower values of correlation coefficients and NMI, across all the sectoral classifications, suggest that asymmetries in bilateral relationships

Downloaded from http://royalsocietypublishing.org/rsos/article-pdf/doi/10.1098/rsos.251246/5646930/rsos.251246.pdf
by guest
on 27 June 2026

Table 1. Comparison of similarity measures between WTN and WEETN across sectors for 1995, 2007 and 2019. Undirected ($\tilde{G}_T, \tilde{G}_C$) and directed (G_T, G_C) networks are compared using Pearson correlation r, Spearman correlation ρ, mutual information $I(X; Y)$ (equation (3.1)) measuring shared information between the two edge weight distributions and normalized mutual information NMI(X, Y) (equation (3.2)). The years chosen span the entire period of the dataset.

sector	year	undirected($\tilde{G}_T, \tilde{G}_C$)				directed(G_T, G_C)			
		r	ρ	$I(X;Y)$	NMI(X,Y)	r	ρ	$I(X;Y)$	NMI(X,Y)
total	1995	0.89	0.96	1.62	0.38	0.81	0.95	1.37	0.33
	2007	0.89	0.97	1.73	0.41	0.80	0.97	1.46	0.35
	2019	0.94	0.97	1.76	0.42	0.91	0.97	1.50	0.36
primary	1995	0.81	0.90	1.15	0.29	0.77	0.89	0.87	0.23
	2007	0.82	0.91	1.16	0.30	0.79	0.89	0.91	0.24
	2019	0.84	0.91	1.23	0.31	0.81	0.90	0.97	0.25
secondary	1995	0.70	0.85	1.19	0.28	0.61	0.84	0.83	0.20
	2007	0.51	0.84	1.05	0.26	0.39	0.83	0.78	0.20
	2019	0.54	0.83	1.15	0.27	0.45	0.82	0.79	0.20
services	1995	0.81	0.96	1.47	0.36	0.78	0.94	1.10	0.28
	2007	0.78	0.96	1.45	0.35	0.73	0.94	1.18	0.30
	2019	0.78	0.95	1.45	0.35	0.73	0.93	1.14	0.28

(e.g. one country being a major exporter but a minor importer) are important for understanding trade-emissions dynamics. In contrast, the undirected representation may mask such directional imbalances, leading to inflated similarity estimates.

To study the inequitable flows of emissions embodied in trade, we construct a network representation that captures the relative environmental burden per unit of trade between countries. We define a new directed network G^{EI} where each edge e_{ij} represents the emissions intensity of trade from country i to country j, measured as the ratio of emissions embodied in trade to trade value

$$e_{ij} = \frac{w^C_{ij}}{w^T_{ij}}, \tag{2.1}$$

where w^T_{ij} and w^C_{ij} are the directed weights in the WTN (G^T) and WEETN (G^C), respectively. This formulation captures the emissions per unit of trade, thereby emphasizing the environmental cost of economic exchange along each link.

We define node-level inequity E_i as the ratio of the total emissions embodied in exports from a country i to its total trade exports:

$$E_i = \frac{\sum_j w^C_{ij}}{\sum_j w^T_{ij}} = \frac{\sum_j e_{ij} w^T_{ij}}{\sum_j w^T_{ij}}, \tag{2.2}$$

where w^C_{ij} and w^T_{ij} denote the directed weights from i to j in the WEETN and WTN, respectively. A value $E_i > 1$ indicates that country i produces a higher share of emissions relative to the value of trade with all its trade partners. We also define an edge-level inequity by considering the ratio of edge weight in G^C with its corresponding edge weight in G^T. To examine the structural footprint of inequity at the local level, we also compute k^{ineq}_i, defined as the number of outgoing edges from i to j that are considered 'inequitable'

$$k^{\text{ineq}}_i = \sum_j \sum_j 1.(e_{ij} > \epsilon) = \sum_j 1.(\frac{w^C_{ij}}{w^T_{ij}} > \epsilon), \tag{2.3}$$

where ϵ is a fixed threshold which is set to 1 to capture strictly inequitable edges and 1.() is the indicator function and e_{ij} is edge-level inequity.

Downloaded from http://royalsocietypublishing.org/rsos/article-pdf/doi/10.1098/rsos.251246/5646930/rsos.251246.pdf
by guest
on 27 June 2026

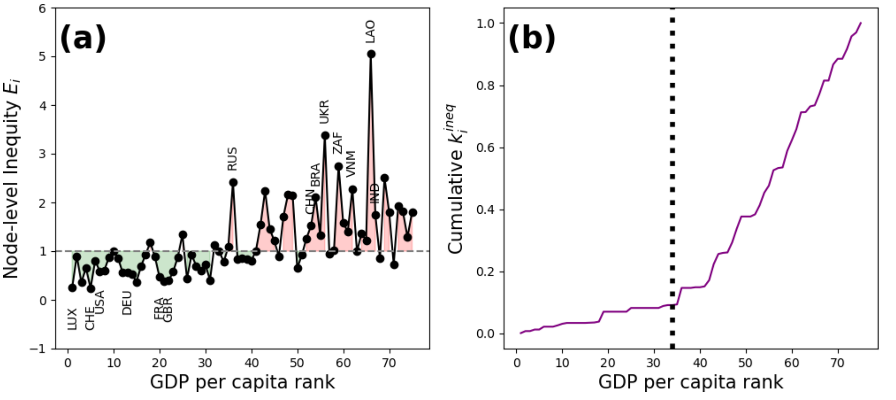

Figure 6. Distribution of E_i and $k^{\mathbf{ineq}}$ against the GDP per capita rank of countries in 2019 (a) shows the values of node level inequity E_i arranged along the x-axis using the GDP per capita ranking of the countries in 2019 from highest to lowest (left to right). Selected countries are labelled to show the distribution. (b) shows the distribution of k_i^{ineq} along the GDP per capita rank. The first incidence of $E_i > 1$ is spotted with Russia (RUS) with the rank of 35 (shown with black dotted line). Beyond this, we can see that there are significant increases in the number of inequitable links that each node has. The GDP per capita data is retrieved from the World Bank (in PPP constant 2021 international) and ranked [23].

First, we examine how E_i and k_i^{ineq} vary between countries ranked by gross domestic product (GDP) per capita. This allows us to assess whether wealthier countries are systematically advantaged in the emissions embodied in trade. We sort countries from richest to poorest and visualize their respective inequity values and the cumulative distribution of inequitable degrees. By comparing E_i and k_i^{ineq} for the year 2019 with our set of 77 countries, it is quite remarkable that this gives a good separation of the nodes into two groups as seen in figure 6a. A higher income group with about 35 members and the rest in the other group. Let us refer to them as Groups H and L. Members of group H have E_i to be less than 1, while the E_i values of group L fluctuate; they are almost always higher than 1. In figure 6b, we can see that the cumulative k_i^{ineq} is plotted against the national income rank, and we can see that the cumulative degree increases substantially as we go towards the lower income countries.

Next, we examine the directionality of these inequitable links. Without resorting to any complex clustering methods, we can define a meaningful grouping by splitting countries into two groups based on their GDP per capita rank: a high-income group (H) and a low-income group (L). A summary of the flows between these groups is listed in table 2. In 2019, we observed that the high-income group (H) accounts for 60% of total trade volume, but only 38% of total emissions embodied in trade. In contrast, the low-income group (L), while engaging in a smaller share of trade, bears a disproportionately larger share of emissions. Notably, L→H edges represent emissions associated with exports from low-income to high-income countries and account for 32% of total emissions, despite making up only 22% of trade volume. Similarly, L→L trade contributes only 18% of trade but results in 30% of emissions.

When comparing these patterns to the year 1995 (based on the same income-based grouping defined using 2019 ranks) we observe a similar but less pronounced asymmetry. At that time, H→H flows accounted for approximately 57% of trade and 37% of emissions, while L→H flows represented about 17% of trade but a notably higher 35% of emissions. In addition, L→L flows made up only 6.6% of trade yet contributed over 15% of emissions. The inequity has not necessarily become more pronounced in terms of L→H emissions intensity, since that proportion dropped slightly. However, what has become more pronounced is the burden of emissions shifting away from high-income countries. The share of total emissions associated with L → L trade has doubled, and overall, the relative emissions shares from low-income country exports have increased, even as their trade share has risen modestly. Table 2 lists a detailed breakdown across three broad sectors over the three years 1995, 2007 and 2019 that span the time period in the dataset.

The temporal analysis of flows across sectors strengthens the case for outsourcing of emissions-intensive activities. For instance, we observe that over the years, the secondary (manufacturing) sector has witnessed a sharp reallocation in emission-intensive production. In 1995, most manufacturing trade occurred within the high-income group (H→ H): 59% of the total, which had fallen to 32% by 2019. For emissions, the same (H→ H) channel dropped from 38% of embodied manufacturing emissions in 1995 to 20% in 2019. During the same period, exports in the secondary sector from the (L) group accounted for 22% of manufacturing trade in 1995 and 43% in 2019. The corresponding change in embodied emissions

Downloaded from http://royalsocietypublishing.org/rsos/article-pdf/doi/10.1098/rsos.251246/5646930/rsos.251246.pdf
by guest
on 27 June 2026

Table 2. Share of total trade and emission embodied in trade flows between high-income (H) and low-income groups in G^T and G^C across sectors for three years 1995, 2007 and 2019: Here the high-income (H) group consists of the top 35 countries when ranked on GDP per capita rank and the rest are classed into the low-income (L) group. Sectors are classified as given in appendix A table 3. The three chosen years span the entire period in the dataset.

		trade			emissions		
sector	direction	1995	2007	2019	1995	2007	2019
total	H → H	0.57	0.45	0.38	0.37	0.26	0.22
	H → L	0.19	0.21	0.22	0.13	0.14	0.16
	L → H	0.17	0.22	0.22	0.35	0.37	0.32
	L → L	0.07	0.12	0.18	0.15	0.23	0.30
primary	H → H	0.39	0.29	0.21	0.26	0.20	0.18
	H → L	0.13	0.15	0.21	0.07	0.08	0.11
	L → H	0.34	0.32	0.21	0.49	0.45	0.31
	L → L	0.14	0.24	0.37	0.18	0.27	0.40
secondary	H → H	0.59	0.43	0.32	0.38	0.26	0.20
	H → L	0.19	0.22	0.25	0.13	0.14	0.15
	L → H	0.15	0.19	0.20	0.33	0.36	0.32
	L → L	0.07	0.15	0.23	0.16	0.24	0.32
services	H → H	0.66	0.62	0.58	0.43	0.35	0.31
	H → L	0.16	0.17	0.18	0.16	0.19	0.22
	L → H	0.14	0.15	0.17	0.31	0.30	0.27
	L → L	0.04	0.06	0.07	0.10	0.15	0.20

is stark, growing from 49% in 1995 to 64% in 2019. In simple terms, approximately two-thirds of manufacturing emissions are tied to exports from L, while those exports make up less than half of manufacturing trade.

To investigate the directionality of inequitable flows in greater detail, we look to assign nodes in the network to a trophic level, a method commonly used in studying ecological networks to detect and visualize the hierarchy and the directionality of the network. Specifically, we use the measure and machinery developed in [24] to measure trophic coherence and assign trophic levels to nodes in our network. We study the directionality in the G^{EI} network in which the edge weights represent the proportional emissions intensity of each trade link. Each directed edge from node i to j is assigned a weight e_{ij} as defined in equation (2.1). We assign heights or trophic levels to the nodes in the network G^{EI} using the measure introduced in [24] that reflects its structural position in the network. Countries with low trophic levels tend to occupy 'upstream' positions, acting as emitters in the global supply chain, while those with higher trophic levels tend to be downstream, importing goods that embody emissions. This hierarchical ordering provides a principled way of visualizing and interpreting the direction of inequitable flows. We also measure the trophic coherence, which measures the extent to which directed edges line up along the hierarchy assigned by the trophic levels. In figure 7a, we have G^{EI} drawn on a hierarchical layout assigned by the trophic levels. The network is pruned to consider only links with weight greater 1, ensuring only inequitable links are shown. The node colours reflect the GDP per capita rank, with warmer colours corresponding to lower-income countries and cooler tones representing the higher-income ones. Lower levels tend to be sources (countries disproportionately responsible for high-emissions exports), and higher levels tend to be sinks (countries accumulating inequitable imports). It can be seen that the countries at the highest level (greater than 1.2) are all those in blue, while those in the lower levels (less than 0.4) are all in shades of red. The trophic coherence is estimated to be approximately 0.38. While this value does not indicate a highly ordered or strictly hierarchical system as would be the case in a perfectly coherent, acyclic network, it is sufficient to suggest the presence of a meaningful global directionality. There is an implicit hierarchy in the network structure.

Downloaded from http://royalsocietypublishing.org/rsos/article-pdf/doi/10.1098/rsos.251246/5646930/rsos.251246.pdf
by guest
on 27 June 2026

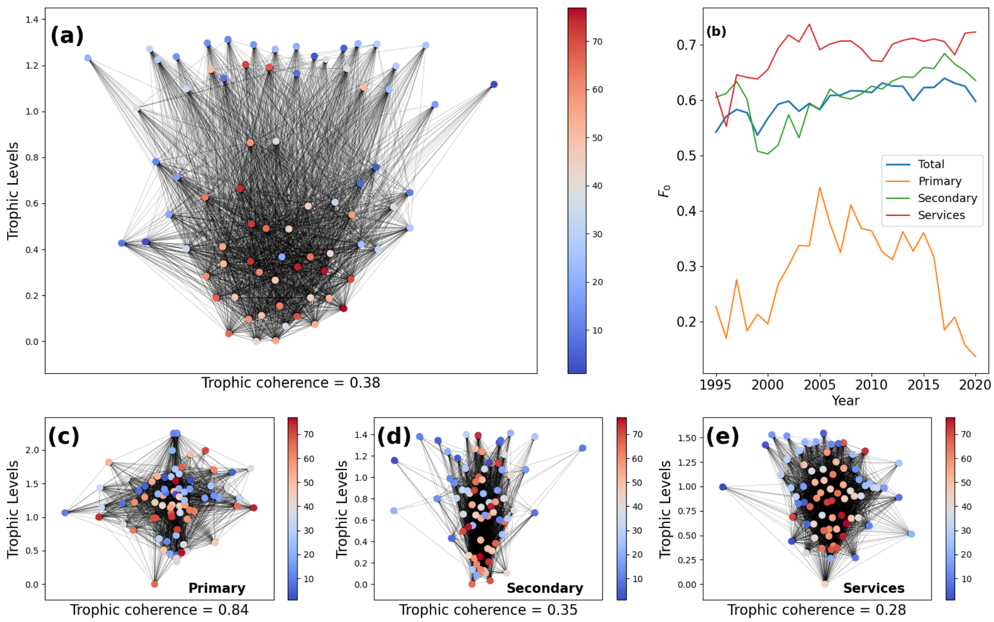

Figure 7. Trophic structure and coherence of G^{EI}: Panel (a) shows the trophic layout of the inequitable emissions network in 2019, using proportional emissions intensity (e_{ij}) as edge weights. Countries are positioned vertically by their trophic levels, with edge directions and node colours indicating the flow of emissions intensity and GDP per capita rank, respectively. Panel (b) presents the evolution of trophic incoherence (F_0) from 1995 to 2020, indicating reducing directionality in total, secondary and services sectors, while the primary sector shows a reversal after 2010. Panels (c)–(e) depict sector-specific trophic structures in 2019 for primary, secondary and services sectors, respectively, each highlighting different degrees of hierarchical organization in the emission-intensive trade patterns.

Countries positioned at the top tend to be the recipients of flows associated with higher emissions per unit of trade from other countries, while the opposite is true for those at the bottom. We find a negative rank correlation of −0.56, indicating that higher-income countries tend to occupy higher trophic positions, while lower-income countries are situated near the bottom of the network. This suggests that emissions-intensive trade disproportionately flows from poorer to wealthier countries. While the correlation could be skewed by a few countries that have a disproportionately high effect on the correlations, a close observation of the network itself offers a strong indication of the role played by income levels. Countries with high trophic levels include affluent European nations such as Germany, the United Kingdom, Sweden, France and Austria, among others. Conversely, countries at the bottom of the trophic hierarchy include Ukraine, Russia, Brazil, Kazakhstan, South Africa, Taiwan, Laos and Vietnam. When disaggregated by sector, the coherence values vary notably: 0.84 for the primary sector, 0.35 for the secondary sector and 0.28 for the services sector. The high coherence in the primary sector suggests a clear and strongly hierarchical direction in the structure of inequitable links. The rank correlations at the sectoral level between the trophic levels and GDP per capita show moderate correlations at −0.39 and −0.29 for secondary and services sectors, respectively, with the primary sector showing a weaker negative correlation. This is because emissions embedded in primary sector trade (such as raw materials, agriculture or extractive industries) may also be influenced by the distribution of natural resource endowments, geophysical conditions and historical patterns of specialization.

Note that the results in figure 7 provide a descriptive analysis similar to results presented in [24]. We measure and report the coherence ($1 - F_0$) values for the observed networks constructed from empirical data alongside external descriptors such as GDP per capita. We do not conduct tests to benchmark these observed values against those of a null model or make claims of causality. We construct unweighted (binary) directed networks of G^{EI} for sectors across all years in the dataset and find that the trophic coherence ($1 - F_0$) is always higher in the weighted G^{EI} networks than the unweighted G^{EI} networks. This suggests that the weight on the flows in G^{EI} only amplifies the directionality in hierarchy. We study the significance and robustness of coherence results for unweighted G^{EI} in appendix D. Constructing appropriately constrained weighted, directed null models for the weighted G^{EI} is not straightforward and is an avenue for future work.

Downloaded from http://royalsocietypublishing.org/rsos/article-pdf/doi/10.1098/rsos.251246/5646930/rsos.251246.pdf
by guest
on 27 June 2026

3. Methods

3.1. Data and network construction

As discussed in §2.1, we construct two weighted networks: WTN (G_T), WEETN (G_C), using the data from OECD ICIO [16] and TeCO2eq [18] databases. These give the total value (in USD for WTN and in tonnes of CO2 for WEETN) of each bilateral trade. The distribution of weights in both networks is large. The smallest non-zero trade volume is less than 1 million USD, and the largest is of the order of 400 billion USD in 2019. The weights in the emissions network are distributed between 0.001 to 500 tonnes of CO2 equivalent. For a meaningful comparison, we normalize the edge weights to obtain $\tilde{G}_T$ and $\tilde{G}_C$ by:

(i) estimating the share of weights. For i and j in network $X \in T, C$ is given by $w_{ij}^X = \frac{W_{ij}^X}{\sum_{i,j} W_{ij}^X}$ where $X = \{T, C\}$.
(ii) symmetrisizing the edge weights to create undirected weighted networks with edges now measuring the total value of the bilateral trade given by $\tilde{w}_{ij}^X = w_{ij}^X + w_{ji}^X$.

For the period 1995–2019, we have bilateral trade flows (and corresponding emissions embodied in these flows) for 77 countries. The networks are complete with all edges having non-zero weights, resulting in a link density of 1. The number of links with very small weights is quite large, whereas only a few links with very large weights exist. The normalization used is uniform throughout the paper, ensuring comparability of results commonly used in the analysis of weighted (and unweighted) trade networks [11,20,25]. The symmetrization used is for the construction of undirected networks, which are compared with directed counterparts.

3.2. Normalized mutual information

Let X and Y be the discrete random variables representing the edge weights from the WTN and WEETN, respectively. The mutual information between them is defined as

$$I(X;Y) = \sum_{x\in X}\sum_{y\in Y} p(x,y)\log\frac{p(x,y)}{p(x)p(y)}, \tag{3.1}$$

where $p(x,y)$, $p(x)$, $p(y)$ are the joint and marginal probability distributions. To ensure the result is scale-independent and lies between 0 and 1, we normalize it using the entropies of the two distributions:

$$NMI(X,Y) = \frac{2I(X;Y)}{H(X)+H(Y)}, \tag{3.2}$$

where $H(X) = -\sum_x p(x)\log(p(x))$ and $H(Y) = -\sum_y p(y)\log(p(y))$. There are several ways to normalize mutual information by the individual entropies [26], and we choose the arithmetic mean of the entropies to avoid any numerical instabilities introduced by very small values of $H(X)$ or $H(Y)$, which may inflate the NMI values.

3.3. Weighted rich club coefficient

We define the rich club as the subset of nodes whose strengths are at least s and write the expression for the rich club coefficient as

$$R_w(s) = \frac{2\sum_i\sum_j w_{ij}}{n_s(n_s-1)}, \tag{3.3}$$

where n_s refers to the number of nodes with strength $s_i > s$. This expression gives the average weight per link among nodes with strength greater than s. However, this definition is insufficient as the uncorrelated random networks have been numerically shown to have rich-club effects. Therefore, this has to be normalized by choosing a null model, generated randomly, to show the significance of the rich-club effect. There have been some choices for the null model put forward in the case of the WTN, we use

$$\rho(s) = \frac{R_w(s)}{R^{\text{null}}(s)}. \tag{3.4}$$

Downloaded from http://royalsocietypublishing.org/rsos/article-pdf/doi/10.1098/rsos.251246/5646930/rsos.251246.pdf
by guest
on 27 June 2026

3.4. Stochastic generative model of trade—null model

In order to choose an appropriate null model, we build on the model in [22], which simulates international trade flows using a preferential attachment mechanism. The model produces weighted and directed networks where countries act as nodes and bilateral trade flows form the edges. It is based on a stochastic process that iteratively places tokens (representing units of trade or emissions) from exporter countries to importer countries based on probabilities of exporters and importers being chosen independently. We summarize the model below:

(i) *Initializing the network*: An initial seed of nodes (σ) are set, which are all connected to each other by edges of weight 1.

(ii) *Node aggregation*: At each time step, the model evaluates whether to add a new exporter or importer node as given in equation (3.5),

$$P_{\text{birth, X}}(t) = \frac{\lambda_X}{N_X(t)}, \tag{3.5}$$

where $X = \{E, I\}$. Here λ_E, λ_I are constants that control how fast exporters and importers grow, and $\sigma_E(t)$, $\sigma_I(t)$ are the active number of nodes exporting and importing in the network. This gives a decreasing probability that ensures slower network growth over time, simulating the saturation of trade relationships. When a new node is added, it is immediately selected for a trade, ensuring integration into the network through an edge created via the preferential attachment rule in the next step.

(iii) *Edge weight aggregation*: If no new node is added, the model instead reinforces existing links by stochastically adding weight (i.e. tokens) between existing nodes. This is done through a gravity-like mechanism, where exporters and importers are selected independently based on their current strengths: s^i_{out}, s^j_{in} which are the total out-strength of node i and total in-strength of node j, respectively (or total exports of i and imports of j). The joint probability of placing a token from i to j is given by

$$s_{i\to j}(t) = P_E(i)\cdot P_I(j) = \frac{(s^i_{out})^\alpha}{\sum_i (s^i_{out})^\alpha}.\frac{(s^j_{in})^\beta}{\sum_j (s^j_{in})^\beta}, \tag{3.6}$$

$$P_{ij} = \frac{s_{i\to j}}{\sum_{ij} s_{i\to j}}. \tag{3.7}$$

(iv) *Weight updat*e: A successful placement increases the edge weight by 1,

$$w_{ij}(t+1) = w_{ij}(t) + 1. \tag{3.8}$$

This continues until the stopping conditions are met: the number of links (non-zero entries in (W) matches the target (L), and the $\sum_{ij} W_{ij}$ matches a target K. In practice, we set $L(\sim 10^6)$ to be large enough such that adding more tokens does not change the in- and out-strengths distributions by less than a small tolerance (ϵ). We also show, in appendix D, that the distribution of strengths for the base case of $\alpha = \beta = 1$ match the distributions seen in the empirical networks, making it suitable without any additional calibration.

Each iteration (or simulation step) places exactly one token, either by forming a link involving a newly added node or by incrementing the weight of an existing edge between two nodes. This means that the total number of simulation steps equals the number of tokens placed, and the progression of the network is driven by this accumulation of tokens. During the early phase of the simulation, many new exporter and importer nodes are added to the network. These node births occur at a relatively high probability, encouraging the model to first construct the broad skeleton of the network structure. As time progresses, however, the probability of introducing new nodes decreases, and the model increasingly focuses on reinforcing existing links by adding weights to them. To ensure realistic dynamics and prevent either node type from dominating too early or too late in the simulation, values of λ are pre-estimated based on the total number of exporters/importers and the seed size. We begin with $\lambda = 0.5$ for simplicity.

Downloaded from http://royalsocietypublishing.org/rsos/article-pdf/doi/10.1098/rsos.251246/5646930/rsos.251246.pdf
by guest
on 27 June 2026

It is also important to note that we make a small modification to the model here to introduce exponents α and β. We use the base case of $\alpha = \beta = 1$ for the null model for simplicity, but we introduce these exponents as they could be tunable parameters to fit the different behaviour in the WTN and WEETN. The model gives a non-symmetric flow matrix, which we symmetrize to create in order to compare it with our weighted undirected WTN (and WEETN). Importantly, we carried a number of distinct simulations varying the parameter alpha and beta. Statistical fitting based on least squares shows that different combinations of alpha and beta are equally similar, proving that $\alpha\beta = 1$ (and therefore the reason we adopted $\alpha\beta = 1$).

The model is stochastic, driven by random node births and probabilistic edge reinforcements—it does not produce a single deterministic network. Instead, each run yields a slightly different realization of the trade network, even with fixed model parameters. In our analysis, we generate 100 such realizations for each sector and year combination. For each realization, the full trade matrix is simulated, then symmetrized and normalized to ensure comparability with the empirical WTN and WEETN. These 100 realizations are used to compute the distribution of the weighted rich-club coefficient, from which we extract the mean and the 10th–90th percentile bounds at each strength threshold. This ensemble-based approach allows us to construct a null model for estimating the normalized rich-club coefficient in figure 5.

For the baseline case where $\alpha = \beta = 1$, it can be shown analytically that in the long-time limit, i.e. $t >> t_f$, where t_f is the time by which all nodes have been introduced, the distribution of edge weights follows $P(w_{ij}) \sim w^{-\eta}$, where $\eta \approx 1.5$, consistent with many results on reinforcement-driven growth processes. See Appendix D for a more detailed analysis.

3.5. Trophic structure and coherence

To quantify the hierarchical structure of a directed, weighted network, we use trophic levels and trophic coherence, following the framework developed in [24,27,28]. For a given directed network G with n nodes and weighted adjacency matrix $W = [w_{ij}]$, where w_{ij} denotes the weight of the directed edge from node i to node j. The trophic level vector h is estimated by solving the system:

$$Lh = v, \tag{3.9}$$

where L is the weighted graph Laplacian operator and v is the vector of node imbalances given by $v_n = w^{\text{in}} - w^{\text{out}}$. Using the levels obtained from solving equation (3.9), the trophic incoherence (F_0) of the network G is calculated by

$$F_0 = \frac{\sum_{ij} w_{ij}(h_j - h_i - 1)^2}{\sum_{ij} w_{ij}}. \tag{3.10}$$

In obtaining h by solving equation (3.9), it is shown that this minimizes $F(h)$ giving the minimum incoherence possible in the network. The trophic coherence is therefore estimated by $1 - F_0$ which is maximum when $F_0 = 0$ and one has a maximally coherent network, which occurs when all level differences $h_j - h_i = 1$ in the network show a perfectly directed hierarchical network. To estimate the trophic coherence, we use the code provided by the authors of [24]. While the methods of trophic analysis are primarily used to study ecological systems, we can see the use of this method to study networks in other fields such as trade, linguistics, neuroscience in [24]. We note that our focus is not on the absolute magnitude of F_0 *per se*, but how direction and hierarchy in the network co-varies with external economic indicators, specifically GDP per capita in our case.

4. Discussion

A central feature of our analysis lies in the way we construct the underlying networks. All undirected and directed networks, whether based on trade value or emissions embodied in trade, are built using normalized flow values, where each link represents a share of a country's total exports. This normalization allows us to focus on the relative structure of trade and emissions flows, abstracting away from absolute magnitudes. In doing so, the resulting networks emphasize who trades with whom and how emissions are distributed across trading partners, rather than how much a country emits or trades in total. This provides meaningful insights into structural asymmetries and inequities, but also means that

Downloaded from http://royalsocietypublishing.org/rsos/article-pdf/doi/10.1098/rsos.251246/5646930/rsos.251246.pdf
by guest
on 27 June 2026

our analysis is less suited to describing aggregate shifts in global trade or emissions over time. Instead, our results highlight distributional patterns and disproportionalities in environmental burden in global trade.

We began our analysis by comparing the undirected networks of trade volume and emissions embodied in bilateral trade. The results indicate a high degree of similarity between the two when measured using both correlation coefficients and NMI. Notably, NMI provides a more robust and stable assessment of similarity compared to correlations, which can be disproportionately influenced by extreme values in the distributions, as evidenced in figure 2b. Among all the networks considered, the total trade volume networks exhibit the highest NMI values, suggesting that, at an aggregate level, the structure of trade and emissions networks is closely aligned. However, when disaggregated into economic sectors, these similarities diminish, reflecting sector-specific divergences in how emissions are embedded in trade. The comparisons become even more nuanced in the case of directed networks, where the direction of flows (exports to imports) matters. These directed networks show a lower alignment between trade and emissions, reinforcing the presence of asymmetries and offering an early indication of the inequitable flows that we explore in greater detail in §2.4.

The analysis also reveals scaling relationships between the product of node strengths and the corresponding edge weights in the emissions and trade networks. These scaling relationships persist over the entire period, showing heavy-tailed distributions in all sectors, as in figures 3 and 4. The exponent γ offers insight into the degree of assortativity in the network—values slightly above 1 suggest that stronger (more connected) nodes tend to be more strongly connected to each other. Our findings indicate that for most sectors, γ hovers slightly above 1, consistent with mild assortative mixing in emissions embedded in trade. However, the primary sector deviates significantly from this pattern, showing distinct tail behaviour and a breakdown of this scaling law in the emissions network. This suggests that emissions in the primary sector may not follow the same structural logic as in trade, reflecting the influence of resource-driven trade patterns rather than economic centrality. These observations are further reinforced by the rich-club coefficient, which again highlights that the primary sector diverges from the secondary and services sectors in how emissions concentrate among high-strength nodes.

Until now, we have referred to inequity in the context of disproportionality and directional asymmetry between trade flows and embodied emissions estimated by statistical measures (e.g. correlations, NMI). While these are descriptive results and do not provide a mechanistic explanation for the emergence of these inequities, they provide a base for further normative studies on this issue. One area of future work would be to build on the literature relating to the emergence of inequitable norms in models of cultural evolution as a possible mechanism to explain the resulting patterns of trade. By their definition, norms are self-enforcing patterns of behaviour. In [29], the authors define that a given norm is a collection of actions that are considered to be in everyone's interest to conform given the expectation that others are going to conform. The results on inequity in emissions embodied in trade are straightforward yet revealing: poorer countries consistently export goods with higher emissions intensity per unit of trade to wealthier countries. This directional asymmetry—where environmental burdens outweigh trade benefits—persists even under simple GDP-based groupings. Trophic coherence analysis further uncovers a hierarchical network structure, placing lower-income countries upstream as emissions sources. These findings show parallels to results of the theoretical model presented in [30,31], which models an evolutionary game theoretic framework of a bargaining game. The paper shows the emergence of inequitable conventions arising from interactions between agents when there are small initial asymmetries in payoffs. The universe of agents is divided into two groups, and the agents benchmark their actions and outcomes against others within their own group. The two groups of agents face a trade-off between their own gains and the burdens imposed on others, and when adaptation is driven by local comparison rather than global coordination, the system can settle into a stable state of unequal conventions. This closely mirrors the dynamics observed in global trade. Developed nations, often already positioned advantageously within the economic hierarchy, have increasingly shifted toward service-based economies and reduced domestic production of emissions-intensive goods. In contrast, developing nations continue to expand industrial activity, bearing a disproportionate share of global emissions. These patterns align with previous studies documenting how net importers tend to increase their imports, while net exporters deepen their export roles—reinforcing existing trade structures over time. It reflects a kind of stratified convention formation: richer countries benchmark their strategies against peers and pursue lower-emission, high-value sectors, while poorer countries prioritize export volume, even at higher environmental cost.

Temporal analysis of the networks suggests that these inequities are growing over time. For instance, we show that there is a shift in dominance of emissions-intensive exports away from the richer countries

Downloaded from http://royalsocietypublishing.org/rsos/article-pdf/doi/10.1098/rsos.251246/5646930/rsos.251246.pdf
by guest
on 27 June 2026

in the secondary (or manufacturing) sector over the period studied. Future work in this aspect includes further analysis in understanding the changes in the portfolio of exports of different countries, and the effect of reducing emission-intensive exports (while possibly increasing such imports) could lead to a richer classification of countries and trading relationships.

Our study and results complement the literature on consumption-based accounting of emissions which has shown how trade reallocates responsibility across borders. This divergence has intensified calls for a shift in how emissions responsibility is attributed. While traditional frameworks like the Kyoto Protocol and the UNFCCC adopt a production-based accounting—where countries are held responsible for emissions generated within their borders—many researchers advocate for a consumption-based approach. This alternative method attributes emissions to the final consumer of goods and services, thereby offering a more equitable picture of global responsibility [32–37].

Finally, the use of national-level data poses important limitations. Countries are treated as uniform, comparable units despite vast differences in population size, geographic area, economic structure, political systems and natural resource endowments. The analysis in this article has focused only on bilateral trade and the emissions embodied in the trade. There is a natural question that follows, to understand how these flows compare with emissions produced for internal consumption in different countries. While there is some analysis (see appendix D) that indicates similar trends, a more rigorous study is required. Future work would greatly benefit from the use of sub-national data on economic activity and emissions profiles to capture more nuanced and meaningful patterns of flows and inequity. Moreover, the framework developed in this study lends itself to several extensions. Recent approaches to modelling international trade relationships focusing on measures of similarity, influence and susceptibility [38] of countries within the global trade system, rather than using bilateral trade, could be useful in uncovering directionality of inequitable flows. For instance, by applying community detection techniques, one could investigate the emergence and stability of inequitable trading blocs. Finally, the null model inspired by the *SynthTrade* model in [22] could be expanded into a coupled generative model of trade and embodied emissions, offering a promising tool for simulating the co-evolution of global trade and GHG emissions.

Ethics. This work did not require ethical approval from a human subject or animal welfare committee.

Data accessibility. All data used in the paper are from publicly available sources. Data used in this paper are primarily from OECD's Inter-country Input Output Tables (ICIO) https://www.oecd.org/sti/ind/inter-country-input-output-tables.html and https://data-explorer.oecd.org/?tm=DF_ICIO_GHG_TRADE_2023 OECD Greenhouse Gas Footprints (GHGFP). Per capita GDP data are retrieved from the World Bank from https://data.worldbank.org/indicator/NY.GDP.PCAP.CD. Some data on the country level emissions are retrieved from the Emissions Database for Global Atmospheric Research (EDGAR) https://edgar.jrc.ec.europa.eu/dataset_ghg70. Data and relevant code for this research work are stored in GitHub: https://github.com/Nk173/Trade-Emissions-Inequity and have been archived within the Zenodo repository [39].

Declaration of AI use. We have not used AI-assisted technologies in creating this article.

Authors' contributions. N.K.: conceptualization, data curation, investigation, visualization, writing—original draft; H.J.J.: supervision, writing—review and editing; E.V.: conceptualization, supervision, writing—review and editing.

All authors gave final approval for publication and agreed to be held accountable for the work performed therein.

Conflict of interest declaration. We declare we have no competing interests.

Funding. No funding has been received for this article.

Appendix A. Sectoral classification

Table 3 provides a mapping of economic activities as listed in the OECD ICIO tables into three broad sectoral categories: primary, secondary and services. This classification facilitates the aggregation of input–output data for macro-sectoral analysis. The activities are grouped based on their standard industry descriptions and aligned with conventional economic sector boundaries.

Appendix B. Trophic coherence for unweighted G^{EI}

The results in figure 8 provide a descriptive analysis of the trophic analysis mentioned in equation (3.10) for the weighted directed network G^{EI}. We assess the statistical significance of the trophic analysis using unweighted directed inequity networks constructed by removing the weights in G^{EI} and keeping only the directions. We benchmark their trophic coherence against a degree-preserving null ensemble generated with the directed configuration model from the NetworkX package [40,41], which randomizes edge pairings while exactly preserving each node's in- and out-degree.

Downloaded from http://royalsocietypublishing.org/rsos/article-pdf/doi/10.1098/rsos.251246/5646930/rsos.251246.pdf
by guest
on 27 June 2026

Table 3. Classification of activities from the OECD ICIO database into primary, secondary and services sectors.

sector	activity
primary	agriculture, hunting, forestry
	fishing and aquaculture
	mining and quarrying, energy-producing products
	mining and quarrying, non-energy-producing products
	mining support service activities
	coke and refined petroleum products
	chemicals and chemical products
	basic pharmaceutical products and pharmaceutical preparations
	rubber and plastics products
	other non-metallic mineral products
	basic metals
	fabricated metal products (except machinery and equipment)
secondary	food products, beverages and tobacco
	textiles, wearing apparel and leather products
	wood and products of wood and cork
	paper products and printing
	computer, electronic and optical equipment
	electrical equipment
	machinery and equipment n.e.c.
	motor vehicles, trailers and semi-trailers
	other transport equipment
	other manufacturing; repair and installation of machinery
	electricity, gas, steam and air conditioning supply
	water supply; sewerage, waste management and remediation
services	construction
	wholesale and retail trade; repair of motor vehicles
	land transport and transport via pipelines
	water transport
	air transport
	warehousing and support activities for transportation
	postal and courier activities
	accommodation and food service activities
	publishing, audiovisual and broadcasting activities
	telecommunications
	IT and other information services
	financial and insurance activities
	real estate activities
	professional, scientific and technical activities

(*Continued.*)

Downloaded from http://royalsocietypublishing.org/rsos/article-pdf/doi/10.1098/rsos.251246/5646930/rsos.251246.pdf
by guest
on 27 June 2026

Table 3. (*Continued.*)

sector	activity
	administrative and support service activities
	public administration and defence; compulsory social security
	education
	human health and social work activities
	arts, entertainment and recreation
	other service activities
	activities of households as employers

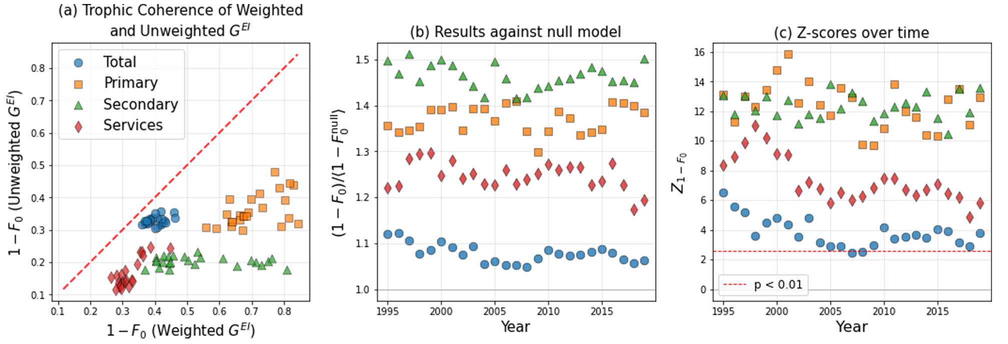

Figure 8. Statistical significance of trophic coherence in unweighted G^{EI} : (a) Scatter plot of the trophic coherence ($1 - F_0$) for the weighted G^{EI} and unweighted G^{EI} for all sectors across all years 1995–2019. (b) Time series of the ratio of $(1 - F_0)/\langle 1 - F_0^{null}\rangle$ where $1 - F_0$ is the trophic coherence of the empirical network and $\langle 1 - F_0^{null}\rangle$ is the mean of the trophic coherence of 100 random networks generated using the directed configuration model. Results for all sectors across the years are presented, showing that the empirical networks for all sectors, over the period 1995–2019, have more coherence than the random networks. Panel (b) shows the Z-scores for the coherence calculated for all sectors over the period 1995–2019. The red dotted line shows the Z-score corresponding to p-value < 0.01 indicating that almost all trophic coherence results (all except the inequity network constructed based on aggregate (or total) trade in 2007 and 2008) are statistically significant. All markers used for different sectors are consistent as in the legend of (a).

For each year and sector, we compute F_0 on the empirical graph and on the null ensemble, reporting the ratio of $(1 - F_0)/\langle 1 - F_0^{null}\rangle$ and Z-scores for $1 - F_0$ (figure 8b,c, respectively). Across all cases, the empirical networks are more coherent than the null, indicating directional hierarchy beyond degree marginals. In general, the coherence values of the weighted networks are higher than the unweighted networks. It is important to note that we do not infer statistical significance for the weighted G^{EI} based on the results of unweighted G^{EI}.

Appendix C. Scaling relationships of national emissions and GDP

In the previous analysis, we considered data pertaining only to bilateral trade. Here, we consider rescaled emissions and GDP data for countries for 1972 and 2022 using data from the Emissions Database for Global Atmospheric Research (EDGAR) [42,43] and the World Bank [23], respectively, which includes total emissions and not just those embodied in trade. We consider the size of an economy by its economic output (given by its GDP). The figure 9a,b show the relationship between emissions and GDP (and their respective per capita quantities). These figures show quantities that are normalized by the respective maximum values and then log-transformed. This process scales both variables between 0 and 1, with the maximum value becoming 1, and then compresses the data using the logarithm. Since the logarithm of a value less than 1 is negative, most normalized values become negative, reflecting how much smaller each country's emissions or GDP is relative to the maximum. This transformation is particularly useful for analysing proportional relationships between countries, as it highlights relative differences more clearly, especially for smaller values. The transformation is shown in equation (C 1) where X_i represents the quantities analysed (emissions, GDP, emissions per capita and GDP per capita):

Downloaded from http://royalsocietypublishing.org/rsos/article-pdf/doi/10.1098/rsos.251246/5646930/rsos.251246.pdf
by guest
on 27 June 2026

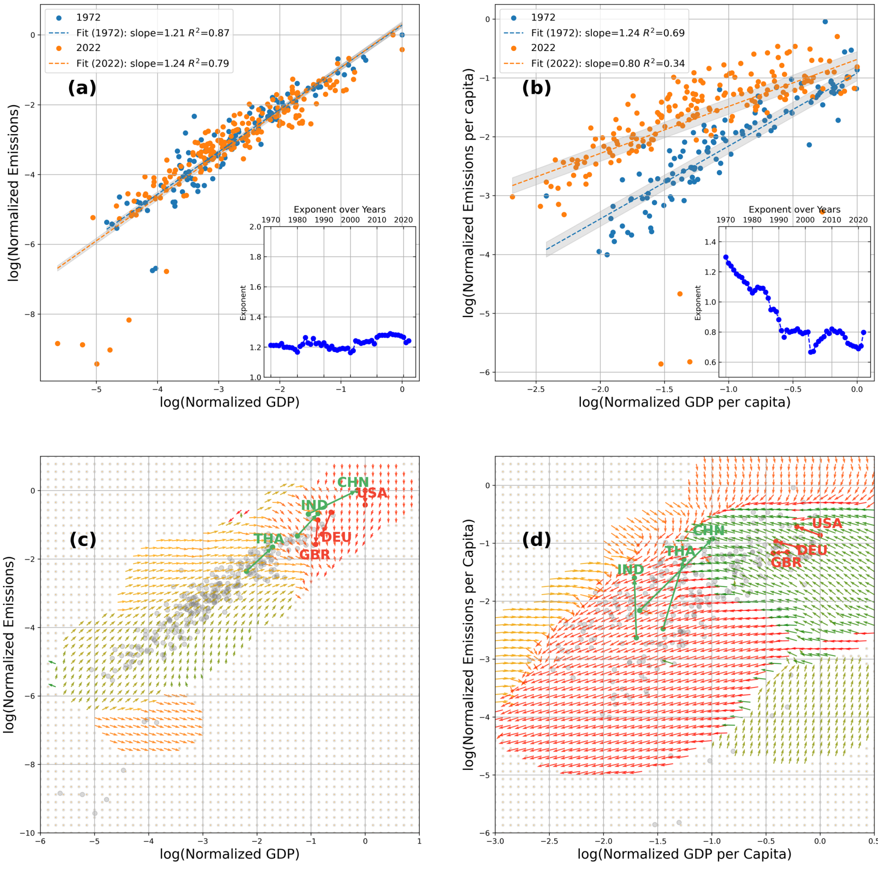

Figure 9. Emissions scaling with GDP**:** Panel (a) shows the relationship between rescaled GDP and emissions using data from countries across 50 years—1972 (in blue) and 2022 (in orange). Panel (b) is a similar plot made per capita estimates of GDP and emissions. All the estimates here are transformed based on (A1). The insets within each plot show the evolution of the exponent β over this period. Emissions data is sourced from [42,43] while GDP is sourced from the World Bank [23]. Panels (c) and (d) present the positions of countries with respect to their rescaled GDP and emissions and rescaled GDP per capita and Emissions per capita, respectively. Both panels (c) and (d) show the field where the arrows point to the average direction of change of countries from their initial position in 1972 to their final position in 2022. The colours reflect the direction of average change as well, with green showing growth in the $x - y$ direction, orange showing growth only in x direction and red showing decline in either direction. We highlight the change in the position of 6 countries with respect to rescaled GDP and rescaled emissions, namely USA, Germany (DEU), United Kingdom (GBR) (also in red), China (CHN), India (IND) and Thailand (THA) (in green).

$$\hat{X}_i = \ln(\frac{X_i}{\max X_i}). \tag{C 1}$$

Fitting the data to curves given by $\hat{e} = k\hat{y}^{\beta}$ show that the rescaled emissions ($\hat{e}$) scales super-linearly with rescaled GDP ($\hat{y}$) with an exponent $\beta \approx 1.2$ suggesting that larger economies are relatively less energy efficient. The inset within figure 9a shows that fitting the data for all years from 1972 to 2022 has a similar exponent. However, when comparing the per capita quantities (as shown in figure 9b on the right-hand side), the relationship seems to have changed over time from a super to sub-linear scaling, with the exponent settling to $\beta \approx 0.8 < 1$ at over the last 20 years (inset within figure 9b).

The average change of different countries based on their position over the 50 year period is calculated, and arrows are drawn to represent the overall direction of change given the position of countries at the start of the period considered. There are two interesting observations: (i) Countries with high GDP are lowering emissions without much change to their GDP. The countries highlighted in red—United Kingdom (GBR), Germany (DEU) and the United States of America (USA)—are shown as examples of this trend, as are other developed economies. (ii) Countries with lower rescaled GDP and emissions show growth in the positive x and y direction. The countries highlighted in green, namely, Thailand (THA), show this trend, as do India (IND) and China (CHN); however, they are relative outliers in their neighbourhood, which consists primarily of richer, developed economies. This is complemented by figure 9d

Downloaded from http://royalsocietypublishing.org/rsos/article-pdf/doi/10.1098/rsos.251246/5646930/rsos.251246.pdf
by guest
on 27 June 2026

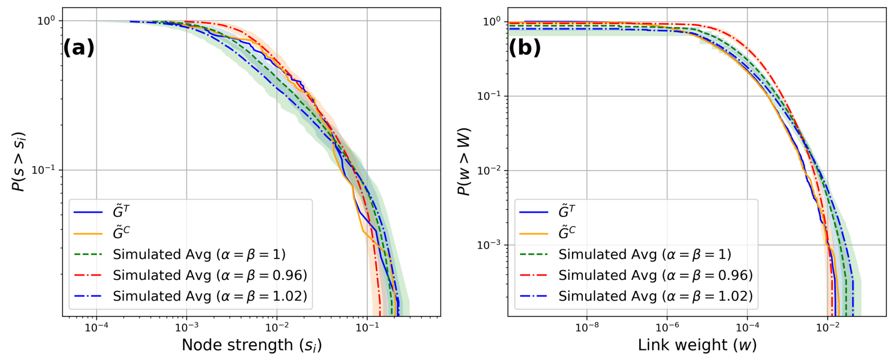

Figure 10. Cumulative distributions of node strength (left) and link weight (right) for the 2019 trade and GHG networks, compared against simulation results from the null model. The base case ($\alpha = \beta = 1$) closely matches the empirical distributions, with additional comparisons shown for $\alpha = \beta = 0.96$. Shaded bands represent variability across 100 simulation runs. The model effectively captures the marginal distribution of strengths and weights, especially for node strength, validating its use as a baseline for analysing structural deviations in network flows.

that shows a similar map with the corresponding per capita estimates. The countries highlighted in red have relatively stabilized the growth in emissions per capita in return for a marginal reduction in GDP per capita, while countries highlighted in green characterize the trend among developing countries with large increases in per capita emissions with marginal growth in per capita GDP. It is noted that China is an outlier given its large change across both emissions and GDP per capita. There is a trend here: wealthier, developed economies are reducing their emissions while showing relatively stable growth, developing economies are increasing emissions exponentially over this period and show varying levels of growth.

Appendix D. Comparing node and link strengths of the simulations of the null model

The objective of plotting the cumulative distributions of node strength and link weights is to evaluate how well the proposed null model reproduces key structural features of real-world trade and emissions networks. We find that these distributions are strikingly similar between the trade and GHG networks, suggesting that the patterns by which economic value and embodied emissions are distributed across countries are closely aligned.

Importantly, the base case of the null model—parameterized by $\alpha = \beta = 1$, replicates these distributions with high accuracy. We compare this with models using $\alpha = \beta = 0.96$ and $\alpha = \beta = 1.02$, and find that, across 100 simulations, the average and range of outputs match the empirical distributions closely. The variance across realizations is also low, reinforcing the reliability of the model (see figure 10). The fit is especially strong for node strength distributions and remains robust, though slightly weaker, for link weight distributions. We find that the null model, while not offering a perfect fit to trade volume flows themselves, provides good fit for the marginal distributions and link weight distribution (less so).

To further support this, we fit the model's parameters to trade and GHG networks across sectors and years. The fitted values consistently fall between 0.92 and 1.02, indicating only minor deviations from the base case. While the fitting process itself is not the main focus of this work, it highlights potential differences between trade and emissions dynamics. A deeper exploration of how these exponents vary—and what they reveal about trade and environmental asymmetries—is a valuable direction for future research. In the present analysis, our goal is to establish that the null model provides a strong and realistic baseline, making it far more appropriate than purely random graph models for studying the global structure of trade and emissions.

References

1. Milanovic B. 2016 *Global inequality: a new approach for the age of globalization*. Cambridge, MA: Harvard University Press. (doi:10.4159/9780674969797)

Downloaded from http://royalsocietypublishing.org/rsos/article-pdf/doi/10.1098/rsos.251246/5646930/rsos.251246.pdf
by guest
on 27 June 2026

2. Burke M, Hsiang SM, Miguel E. 2015 Global non-linear effect of temperature on economic production. *Nature* **527**, 235–239. (doi:10.1038/nature15725)
3. Dell M, Jones BF, Olken BA. 2012 Temperature shocks and economic growth: evidence from the last half century. *Am. Econ. J.* **4**, 66–95. (doi:10.1257/mac.4.3.66)
4. Chancel L. 2022 Global carbon inequality over 1990–2019. *Nat. Sustain*. **5**, 931–938. (doi:10.1038/s41893-022-00955-z)
5. Piketty T, Saez E. 2014 Inequality in the long run. *Science* **344**, 838–843. (doi:10.1126/science.1251936)
6. Friedlingstein P *et al*. 2023 Global carbon budget 2023. *Earth Syst. Sci. Data* **15**, 5301–5369. (doi:10.5194/essd-15-5301-2023)
7. Serrano MA, Boguñá M. 2003 Topology of the world trade web. *Phys. Rev. E. Stat. Nonlin. Soft Matter Phys*. **68**, 015101. (doi:10.1103/PhysRevE.68.015101)
8. Garlaschelli D, Loffredo MI. 2004 Fitness-dependent topological properties of the world trade web. *Phys. Rev. Lett*. **93**, 188701. (doi:10.1103/PhysRevLett.93.188701)
9. Di Vece M, Garlaschelli D, Squartini T. 2022 Gravity models of networks: integrating maximum-entropy and econometric approaches. *Phys. Rev. Res.* **4**, 033105. (doi:10.1103/PhysRevResearch.4.033105)
10. Garlaschelli D, Loffredo MI. 2005 Structure and evolution of the world trade network. *Physica A* **355**, 138–144. (doi:10.1016/j.physa.2005.02.075)
11. Bhattacharya K, Mukherjee G, Saramäki J, Kaski K, Manna SS. 2008 The international trade network: weighted network analysis and modelling. *J. Stat. Mech*. **2008**, 02002. (doi:10.1088/1742-5468/2008/02/P02002)
12. Fagiolo G, Reyes J, Schiavo S. 2009 World-trade web: topological properties, dynamics, and evolution. *Phys. Rev. E. Stat. Nonlin. Soft Matter Phys*. **79**, 036115. (doi:10.1103/PhysRevE.79.036115)
13. Hertwich EG, Peters GP. 2009 Carbon footprint of nations: a global, trade-linked analysis. *Environ. Sci. Technol*. **43**, 6414–6420. (doi:10.1021/es803496a)
14. Liu Y, Ma R, Guan C, Chen B, Zhang B. 2022 Global trade network and CH4 emission outsourcing. *Sci. Total Environ.* **803**, 150008. (doi:10.1016/j.scitotenv.2021.150008)
15. Guidi G, Mastrandrea R, Facchini A, Squartini T, Kennedy C. 2024 Tracing two decades of carbon emissions using a network approach. *Sci. Rep*. **14**, 7251. (doi:10.1038/s41598-024-57351-0)
16. OECD. 2025 OECD Inter-Country Input-Output Tables. See http://oe.cd/icio.
17. Yamano N, Alsamawi A, Webb C, Cimper A, Zürcher C, Chiapin Pechansky R. 2023 *Development of the OECD inter country input-output database 2023*.
18. OECD. 2023 Greenhouse gas footprints (GHGFP): emissions embodied in bilateral trade. OECD Data Explorer. See https://data-explorer.oecd.org/?tm=DF_ICIO_GHG_TRADE_2023 (accessed 01 June 2025)
19. Yamano N, Guilhoto J. 2020 *CO2 emissions embodied in international trade and domestic final demand: methodology and results using the OECD inter-country input-output database*.
20. Squartini T, Fagiolo G, Garlaschelli D. 2011 Randomizing world trade. II. A weighted network analysis. *Phys. Rev. E. Stat. Nonlin. Soft Matter Phys*. **84**, 046118. (doi:10.1103/PhysRevE.84.046118)
21. Squartini T, Fagiolo G, Garlaschelli D. 2011 Randomizing world trade. I. A binary network analysis. *Phys. Rev. E. Stat. Nonlin. Soft Matter Phys*. **84**, 046117. (doi:10.1103/PhysRevE.84.046117)
22. García-Algarra J, Mouronte-López ML, Galeano J. 2019 A stochastic generative model of the world trade network. *Sci. Rep*. **9**, 18539. (doi:10.1038/s41598-019-54979-1)
23. World Bank. 2025 GDP per capita (current USD). See https://data.worldbank.org/indicator/NY.GDP.PCAP.CD (accessed 01 June 2025)
24. MacKay RS, Johnson S, Sansom B. 2020 How directed is a directed network? *R. Soc. Open Sci*. **7**, 201138. (doi:10.1098/rsos.201138)
25. Mastrandrea R, Squartini T, Fagiolo G, Garlaschelli D. 2014 Reconstructing the world trade multiplex: the role of intensive and extensive biases. *Phys. Rev. E. Stat. Nonlin. Soft Matter Phys*. **90**, 062804. (doi:10.1103/PhysRevE.90.062804)
26. Nguyen X, Epps J, Bailey J. 2010 Information theoretic measures for clusterings comparison: variants, properties, normalization and correction for chance. *J. Mach. Learn. Res* **11**, 2837–2854. (doi:10.5555/1756006.1953024)
27. Johnson S, Domínguez-García V, Donetti L, Muñoz MA. 2014 Trophic coherence determines food-web stability. *Proc. Natl Acad. Sci. USA* **111**, 17923–17928. (doi:10.1073/pnas.1409077111)
28. Johnson S, Jones NS. 2017 Looplessness in networks is linked to trophic coherence. *Proc. Natl Acad. Sci. USA* **114**, 5618–5623. (doi:10.1073/pnas.1613786114)
29. Axtell RL, Epstein JM, Young HP. 2012 Chapter 8. The emergence of classes in a multi-agent bargaining model. In *Generative social science: studies in agent-based computational modeling* (ed. JM Epstein), pp. 177–195. Princeton, NJ, USA: Princeton University Press. (doi:10.1515/9781400842872.177)
30. Cochran C, O'Connor C. 2019 Inequality and inequity in the emergence of conventions. *Politics Philos. Econ*. **18**, 264–281. (doi:10.1177/1470594X19828371)
31. O'Connor C. 2019 Social categories, coordination, and inequity. In *The origins of unfairness*, pp. 40–57. Oxford, UK: Oxford University Press. (doi:10.1093/oso/9780198789970.003.0003)
32. Davis SJ, Peters GP, Caldeira K. 2011 The supply chain of CO2 emissions. *Proc. Natl Acad. Sci. USA* **108**, 18554–18559. (doi:10.1073/pnas.1107409108)
33. Davis SJ, Caldeira K. 2010 Consumption-based accounting of CO2 emissions. *Proc. Natl Acad. Sci. USA* **107**, 5687–5692. (doi:10.1073/pnas.0906974107)

Downloaded from http://royalsocietypublishing.org/rsos/article-pdf/doi/10.1098/rsos.251246/5646930/rsos.251246.pdf
by guest
on 27 June 2026

34. Kanemoto K, Moran D, Lenzen M, Geschke A. 2014 International trade undermines national emission reduction targets: new evidence from air pollution. *Glob. Environ. Change* **24**, 52–59. (doi:10.1016/j.gloenvcha.2013.09.008)
35. Peters GP, Minx JC, Weber CL, Edenhofer O. 2011 Growth in emission transfers via international trade from 1990 to 2008. *Proc. Natl Acad. Sci. USA* **108**, 8903–8908. (doi:10.1073/pnas.1006388108)
36. Raupach MR *et al*. 2014 Sharing a quota on cumulative carbon emissions. *Nat. Clim. Chang*. **4**, 873–879. (doi:10.1038/nclimate2384)
37. Peters GP, Hertwich EG. 2008 CO2 embodied in international trade with implications for global climate policy. *Environ. Sci. Technol*. **42**, 1401–1407. (doi:10.1021/es072023k)
38. Kumar N, Jensen HJ, Viegas E. 2023 Economic trading susceptibility: constructing networks of mutual influence through the fitness of countries. *Entropy* **25**, 141. (doi:10.3390/e25010141)
39. Kumar N. 2025 Nk173/trade-emissions-inequity: trade-inequity (v1.0). Zenodo (doi:10.5281/zenodo.17459334)
40. Hagberg AA, Schult DA, Swart PJ. 2008 Exploring network structure, dynamics, and function using networkX (eds G Varoquaux, T Vaught, J Millman). In *Python in Science Conference*, Pasadena, California, pp. 11–15. Pasadena, CA USA: SciPy. (doi:10.25080/TCWV9851)
41. Newman ME, Strogatz SH, Watts DJ. 2001 Random graphs with arbitrary degree distributions and their applications. *Phys. Rev. E. Stat. Nonlin. Soft Matter Phys*. **64**, 026118. (doi:10.1103/PhysRevE.64.026118)
42. Crippa M *et al*. 2024 *GHG emissions all world countries*. Luxembourg: Publications Office European Union.
43. European Commission, Joint Research Centre JRC, & International Energy Agency IEA. 2022 IEA-EDGAR CO2 (v4), a component of the EDGAR community GHG database (EDGAR_2025_GHG). See https://edgar.jrc.ec.europa.eu/dataset_ ghg70 (accessed 26 June 2025)

Downloaded from http://royalsocietypublishing.org/rsos/article-pdf/doi/10.1098/rsos.251246/5646930/rsos.251246.pdf
by guest
on 27 June 2026